

FATIGUE STRENGTH OF AL-ALLOYS IN CASE OF RANDOM SPECTRA LOADING

G. I. Nesterenko, V. N. Basov

Central Aerohydrodynamic Institute (TsAGI). Russia

Abstract

This paper presents the results of fatigue strength study of Al-alloys D16AT, 2024-T3, 1163T7 and 2324-T39 in case of random loading spectra of transport aircraft lower wing surface. Tests were carried out on the flat specimens with central hole. Test programs were the modified TWIST standardized loading sequence, Russian transport airplane (RTJ) and Boeing 767 wing loading programs.

1. Introduction

The problem of aircraft structure fatigue becomes very important due to the increase in stress levels in the primary structural elements as well as to the required large lifetime of the aircraft. According to the aviation regulations of the Inter-state Aviation Committee (MAK) the fatigue strength of a structure should be ensured considering the design goal [1] in the design stage. Fatigue characteristics of the critical locations in structure should be found for the typical in-service load spectra. It is recommended to define the threshold interval in terms of fatigue strength. Attention should be paid to the selection of the appropriate material.

The solution of the fatigue problems is impeded by the strong dependence of fatigue life versus various factors including the alloy composition, loading spectrum, significant fatigue life scattering. Attainment of high weight efficiency of aircraft structures requires more thorough investigations in fatigue behaviour of Al-alloys, which are the major alloys in the contemporary aircraft structures. This paper includes some tests aimed to solve the problems mentioned.

2. Test procedure

Fatigue characteristics of Al-alloys D16AT, 1163T7, 2024-T3 and 2324-T39 were examined. The first two alloys are applied in lower wing structures of Russian airplanes while next two are typical for the lower wings of Boeing airplanes. The traditional alloys D16AT and 2024-T3 were used in the structures of aging airplanes; the alloys 1163T7 and 2324-T39 are used in the structures of contemporary airplanes. The traditional alloys contain more Si and Fe as compared to the improved alloys. The percentage of these impurities was determined in Russian Institute of Aviation Materials (VIAM) (Table 1). The characteristics of strength of these materials are outlined in the Table 2 basing on the results of standardized tests.

Tensile fatigue strength was studied on the specimens in a form of stripe with a hole (Fig. 1). The specimens were 4.1 mm thick for 2024-T3; 6 mm thick for D16AT; 8 mm for 1163T7 and 2324-T39. Stress concentrator in the form of the hole makes the alloy behaviour while specimen tests close to those in the structure operation [2]. Stress concentration factor along the gross section of this specimen is $K_t = 3.1$.

The tests were conducted on Schenck electrohydraulic machine PSA-10 with computer control. Macrocracks detection and observation in the tests was made by means of an eddy-current device VDM-1 [3] providing the measurements of cracks in the range of $0.1 \div 8 \text{ mm}^2$. The initiation and growth of macrocracks were analysed by quantitative fractography [4] after the specimen failure. Fractographic analysis of the crack surfaces was performed using the electronic microscope Cwikscan 50A, which have the resolution of 50 \AA . The size of initial cracks measured by fractographic method was 0.7 mm.

The specimens were tested under regular (pulsating) and irregular (random) loading. Regular loading was sine one with the stress ratio $R=0$. Loading frequency was 2-3 Hz. The irregular loadings were the programs of lower wing surface loading for the wide-body RTJ [5], wide-body Boeing 767 [6] and also modified load sequence TWIST [7], named Truncated TWIST.

Standardized TWIST program was generated basing on the measured load spectra for narrow-body airplanes F-28, Boeing 720 and Caravella. Random loading was simulated using the complex software SAMUM developed in TsAGI. Irregular loading frequency was variable, inversely proportional to the load amplitude to provide within 2-22 Hz approximately the same loading rates, equal to those for the zero-to-tension cycle with $\sigma_{max}=133$ Mpa.

3. Fatigue curves

Experimental fatigue curves were obtained for both regular and irregular loading cases. The value of maximum stress in case of irregular loading varied within 70÷220 MPa. The Wohler's curve is shown in Figure 2. The major part of testing was conducted at the maximum gross stress $\sigma_{max}=133$ MPa. Such level of maximum stresses at $R=0$ is widely used to compare the aircraft Al-alloys fatigue characteristics.

While construction of the fatigue curves for irregular loading the value of mean stress σ_{mean} , which corresponds to the cruise flight with load factor $n_y=1$, was varied. Typical stress diagrams of one of the flights from each loading sequence are presented in Figs. 3-5. Boeing 767 loading program, initially generated by Boeing Co, was in the form of blocks, which consisted of the quasi-random sequence of five different flight types with total 5,000 flights in one block. The RTJ program had 4,000 flights of ten types in each flight block. Truncated TWIST was derived from TWIST program by truncating maximum loads higher than $2.15 \cdot \sigma_{mean}$. The simulation of Truncated TWIST was represented by flight block of 4,000 flights. One block was of ten flight types differed in extreme load values and their amount.

Fatigue curves in case of irregular loading were plotted in *mean flight stress*, σ_{mean} , vs. *number of flights*, N (Figs. 6-8). Stresses σ_{mean} varied in the range of 60÷120 MPa. The fatigue failure behaviour of the alloy in case of random loading were analysed for σ_{mean} mentioned, as well as for the typical stresses $\sigma_{mean}=85$ MPa in the lower wing surfaces of transport airplanes.

To compare the stress loading in the specimens (structures) in case of the load programs described (Figs. 3-5) the values of maximum stress σ_{equiv} of the equivalent zero-to-tension cycle were determined for these programs at mean stress of $\sigma_{mean}=85$ MPa. Damage accumulation of the structure during one equivalent zero-to-tension cycle ($R=0$) is equal to that for all the stress cycles in one average statistic flight in terms of damage capability. Damage capability of the average statistic flight is defined as damage during the whole block divided by the number of flights in this block.

The value of σ_{equiv} is found as follows [8]. The set of complete stress cycles of each flight block is replaced by the population of zero-to-tension cycles with maximum stresses calculated as:

$$\sigma_{0i} = \sqrt{2\sigma_{ai} \cdot \sigma_{maxi}} \quad (1)$$

where σ_{ai} – stress amplitude; σ_{maxi} – maximum stress of the i -th cycle in flight block

The value of the maximum stress in the equivalent zero-to-tension cycle is equal to:

$$\sigma_{equiv} = \sqrt[m]{\frac{1}{K} \sum_i (\sigma_{0i})^m} \quad (2)$$

where:

K – number of flights in one flight block;

m – exponent in the fatigue curve equation $\sigma^m N = const$, and the summing is for all particular equivalent zero-to-tension cycles of the flight block.

It is assumed here that $m = 4$.

Equivalent stresses of three load sequences with the mean stresses of $\sigma_m=85$ MPa are presented in Table 3.

4 Durability depending on alloy composition and load level.

Investigations demonstrated the significant effect of the alloy composition and loading level on the material ranking in terms of fatigue.

The durability of plates of improved 1163T7 exceeded approximately in 2 times that of traditional D16AT sheets in case of zero-to-tension loading at $\sigma_{max}=133$ MPa (Fig. 2).

The most severe sequence of random loading is the truncated TWIST, while the less severe one is that for Boeing 767 (Figs. 6-9).

Relation between durability of two alloys compared depends on the program and level of loading. For instance, the durability ratio of 1163T7 plate to D16AT sheet is equal to: 2 – for truncated TWIST; 4 – for RTJ sequence; and 6 for Boeing 767 sequence with mean stresses $\sigma_{mean}=85$ MPa (Fig. 9).

The ratio of 2024-T3 sheets to D16AT sheets lies within 1.25-3.85 range depending on the loading type and level (Fig. 10).

5 Values of accumulated damages at failure

While analysing the aircraft structure life according to the linear hypothesis of Palmgren-Miner the quantity of accumulated damage A should be assigned for failure typical for the given type of loading. Here A was calculated for the loading sequences under study as:

$$A = \frac{\bar{N}}{K} \left(\sum_i \frac{n_i}{N_i} \right)_{block} \quad (3)$$

where

- \bar{N} – mean flight life, taken from tests, (Figs. 6-8),
- K – flight number in one flight block;
- n_i – number of cycles with σ_i stress in one block; σ_i stresses have been recalculated into zero-to-tension stresses σ_{0i} , using (1);
- N_i – number of cycles before failure under σ_{0i} stresses

N_i was determined from fatigue curves with $R=0$ (Fig. 2).

It follows from test-analytical research that A strongly depends on the alloy, loading sequence and mean stress values σ_{mean} in the cruise flight (Fig. 11). At $\sigma_{mean}=85$ MPa the value of A lies within 0.25– 0.55 (Fig. 12). Parameter A is equal to 1.1 for 2024-T3 sheets loaded with Truncated TWIST with $\sigma_{mean}=85$ MPa.

Presented data demonstrate that under certain loading sequences and levels the improved 1163T7 and 2324-T39 alloys have smaller A as compared to the traditional alloys.

6 Durability scatter

While determining the safe life and inspection threshold for aluminium alloy structures the typical scatter factors, such as root-mean-square deviation of life logarithm $S_{lgN}=0.15$, are used [1]. Experimental S_{lgN} values from this study are shown in Fig. 13. For zero-to-tension loading with $\sigma_{max}=133$ MPa of 2024-T3 sheets $S_{lgN}=0.098$, and for Truncated TWIST with $\sigma_{mean}=85$ MPa it is $S_{lgN}=0.058$. Thus, for traditional alloys D16AT and 2024-T3 the value of S_{lgN} is less than 0.15, while for improved alloys it is $S_{lgN}>0.15$.

7 Two stages of fatigue failure

Usually the process of fatigue failure is divided into two stages. The first stage includes the growth of microcracks under the action of shear stresses. The first stage is completed when the microcracks are combined into macrocrack some tenth of a millimeter in size. Macrocracks are growing under conditions of normal breakaway. Often, at the beginning of the second stage, the elements with stress concentration have several fatigue cracks growing, and some of them stop growing while one crack becomes the leading macrocrack [9]. The second stage can be analyzed using the methods of linear fracture mechanics.

In 80-90's, a method to predict fatigue life was developed basing on the theory of small cracks [10]. In this method, the entire process of fatigue failure is presented by the only curve of crack growth, which can be described by

fracture mechanics in terms of stress intensity factor. The initial flaws in Al-alloy materials are replaced by the initial crack of 6-10 microns [10].

The initiation and growth duration of macrocracks were defined in this paper using the methods mentioned above (Figs. 14-17). For the stress loading typical to contemporary transport airplanes, the ratio of macrocrack growth duration to the total specimen life till failure is 10÷30%. Significant difference in scattering between the life till complete failure and macrocrack growth duration should be noted. The ratio of maximum to minimum life till the complete specimen failure lies within the range of $N_{fr_max}/N_{fr_min} \approx 2\div 2.7$. The ratio of maximum to minimum macrocrack growth time lies within the range $N_{cr_max}/N_{cr_min} \approx 2\div 2.7$

In general, the data analysis outlined in Figs. 14-17 discovers some difficulties to describe the whole process of fatigue failure by the unified curve, obtained by methods of linear fracture mechanics.

8 Conclusion

Experimental research on fatigue strength of the aluminium alloys D16AT, 2024-T3, 1163T7, 2324-T39 in case of typical random loading of wing lower surface, such as Truncated TWIST, RTJ and Boeing 767 load programs, shows that:

- For the equal mean stress level the most severe loading is the Truncated TWIST, while the sequence for Boeing 767 is the least severe.
- The durability of aluminium alloys depends on the sequence and level of loading.
- The values of accumulated damages as at failure are within 0.25-2.55 range.
- The fatigue life scattering for traditional aluminium alloys D16AT and 2024-T3 is lower than the standardized one, while the fatigue life scattering for the improved alloys 1163T7 and 2324-T39 is higher than the standardized fatigue scatter. Scattering in macrocrack growth duration

is significantly lower than fatigue scatter till the initiation of macrocracks.

- Macrocrack growth duration is about 10÷30% of fatigue life till failure of specimens with a hole.

References

- [1] Method of Compliance (MOC) "Ensuring safety of structure in terms of strength during long-term operation" Add. Aviation Regulations AP25.571. AR MAK. 1996 (in Russian).
- [2] Marin N.I. "Static endurance of aircraft structural elements". Mashinostroyeniye, Moscow, 1968, - 162 pp. (in Russian).
- [3] Zverev Ye.A., Kononov V.V., Yablonsky I.S. "Methods to study life of specimens with small cracks". "Zavodskaya Laboratoriya" Journal, N 1, v.52, 1986. p.71-74 (in Russian).
- [4] Stoyda Yu.M. "Development of quantitative fractography method and investigation into crack resistance of Al-alloy structural elements" Abstract to the Ph. D. thesis, VIAM. 1988 (in Russian).
- [5] Basov V.N., Nesterenko G.I., Strizhius V.Ye. "Standardized loading sequence for heavy transport wing", Trudy TsAGI, issue 2642, Moscow 2001, p.26-34 (in Russian).
- [6] Fowler R.F., and Watanabe R.T. "Development of jet transport airframe test spectra", Boeing Commercial Airplanes, Seattle, Washington, USA, May 1989, -16 pp.
- [7] DeJonge J.B., Schütz D., Lowak H., Schijve J. "A standardized load sequence for flight simulation tests on transport aircraft wing structures", LBF Bericht FB-106 (NLR 73029 U), 1973.
- [8] Vorobjov A.Z., Leybov V.G., Olkin B.L., Stebenev V.N. "Ensuring enhanced lifetime for wide-body aircraft", in: "Aircraft Structural Strength", Mashinostroyeniye, Moscow, 1982, p.122-151 (in Russian).
- [9] Vorobjov A.Z., Olkin B.I., Stebenev V.N., Rodchenko T.S. "Fatigue strength of structural elements". Mashinostroyeniye, Moscow, 1990, - 240 pp. (in Russian).
- [10] Newman J Jr. "Advances in fatigue and fracture mechanics analysis for aircraft structures", Langley Research Center, Proceedings of the 20th Symposium of ICAF, July 14-16, 1999, Bellevue, Washington, USA, Vol.1, p.3-42.

FATIGUE STRENGTH OF AL-ALLOYS IN CASE OF RANDOM SPECTRA LOADING

Table 1 Aluminium alloys composition: Si and Fe content

Alloy	D16AT clad sheet	2024-T3 sheet	1163T7 plate	2324-T39 plate
Si, %	0.22	0.1	0.01-0.1	0.04
Fe, %	0.31	0.25	0.05-0.15	0.1

Table 2 Alloy average strength values

Alloy	D16AT, clad sheet	2024-T3 sheet	1163T7 plate	2324-T39 plate
Yield strength $\sigma_{0.2}$, MPa	347	379	402	467
Ultimate strength σ_U , MPa	446	483	510	504

Table 3 Equivalent stresses of average statistical flight at $\sigma_{mean} = 85$ MPa

Loading program	σ_{equiv} , MPa	n_y^{max}
RTJ	170	1.91
Boeing 767	151	2.10
Truncated TWIST	220	2.15

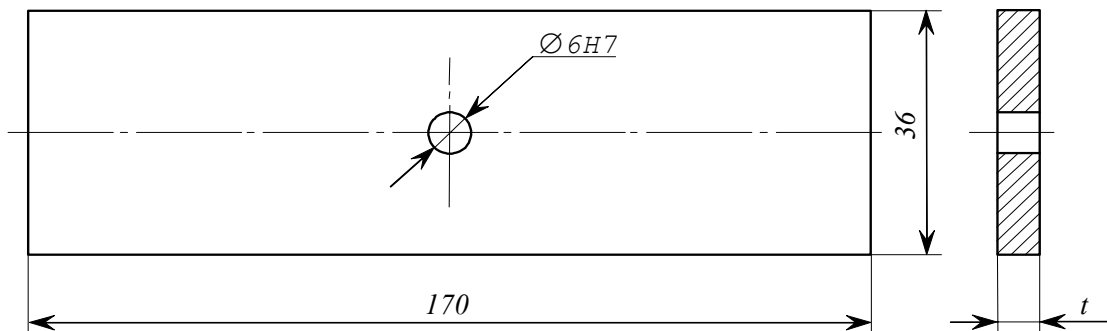


Fig. 1. Specimen for fatigue tests

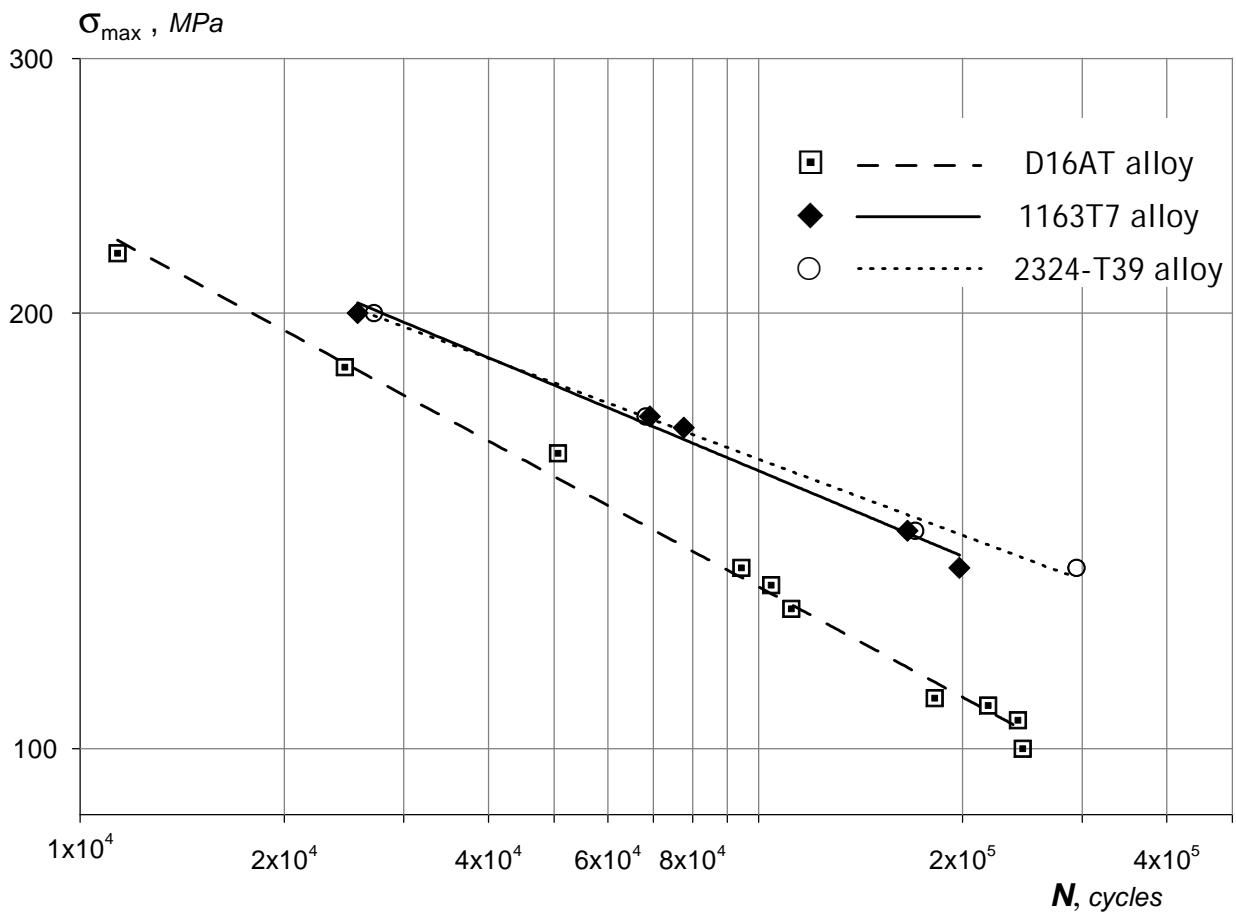


Fig. 2. Fatigue curves for D16AT, 1163T7 and 2324-T39 under zero-to-tension loading

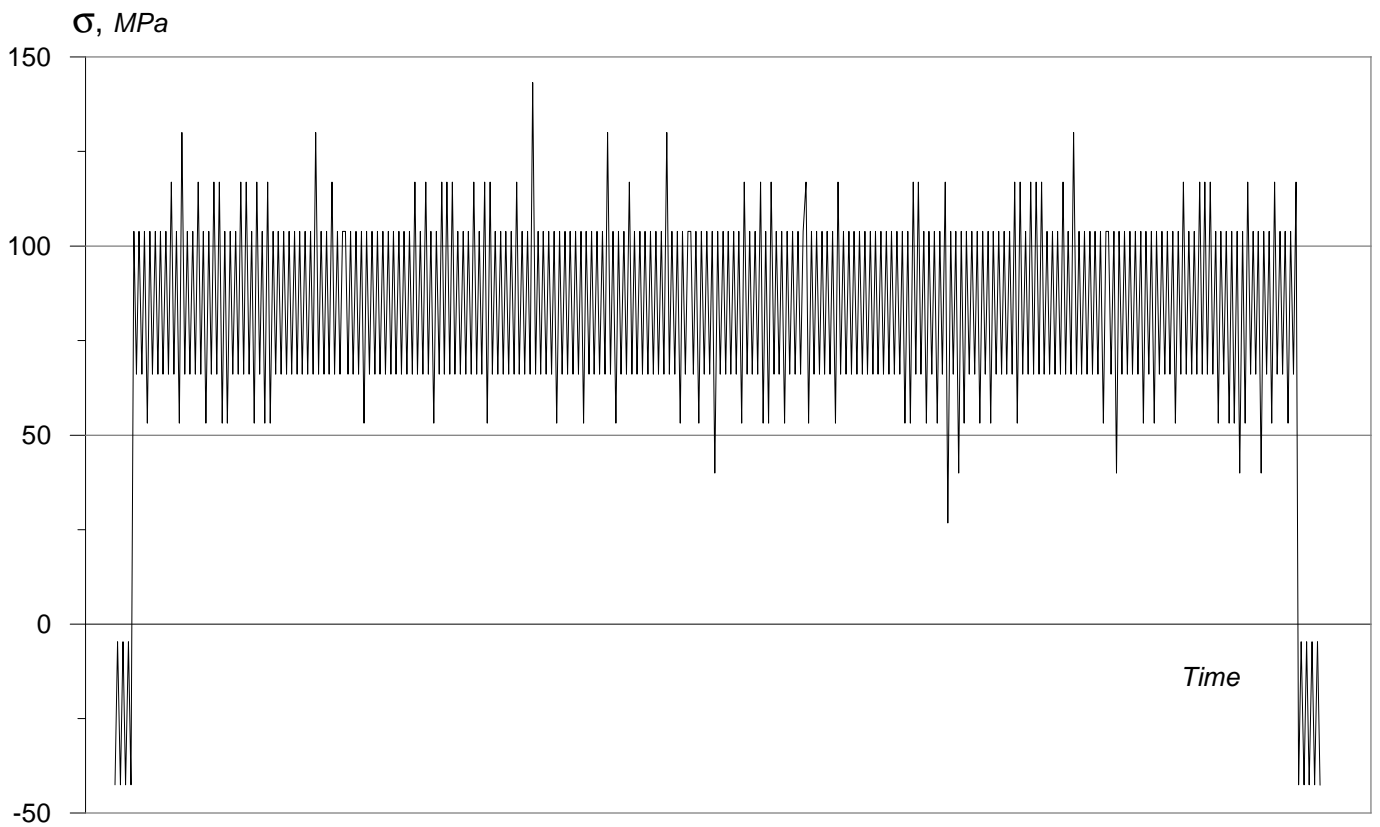


Fig. 3. Typical stress cyclogram for Truncated TWIST sequence

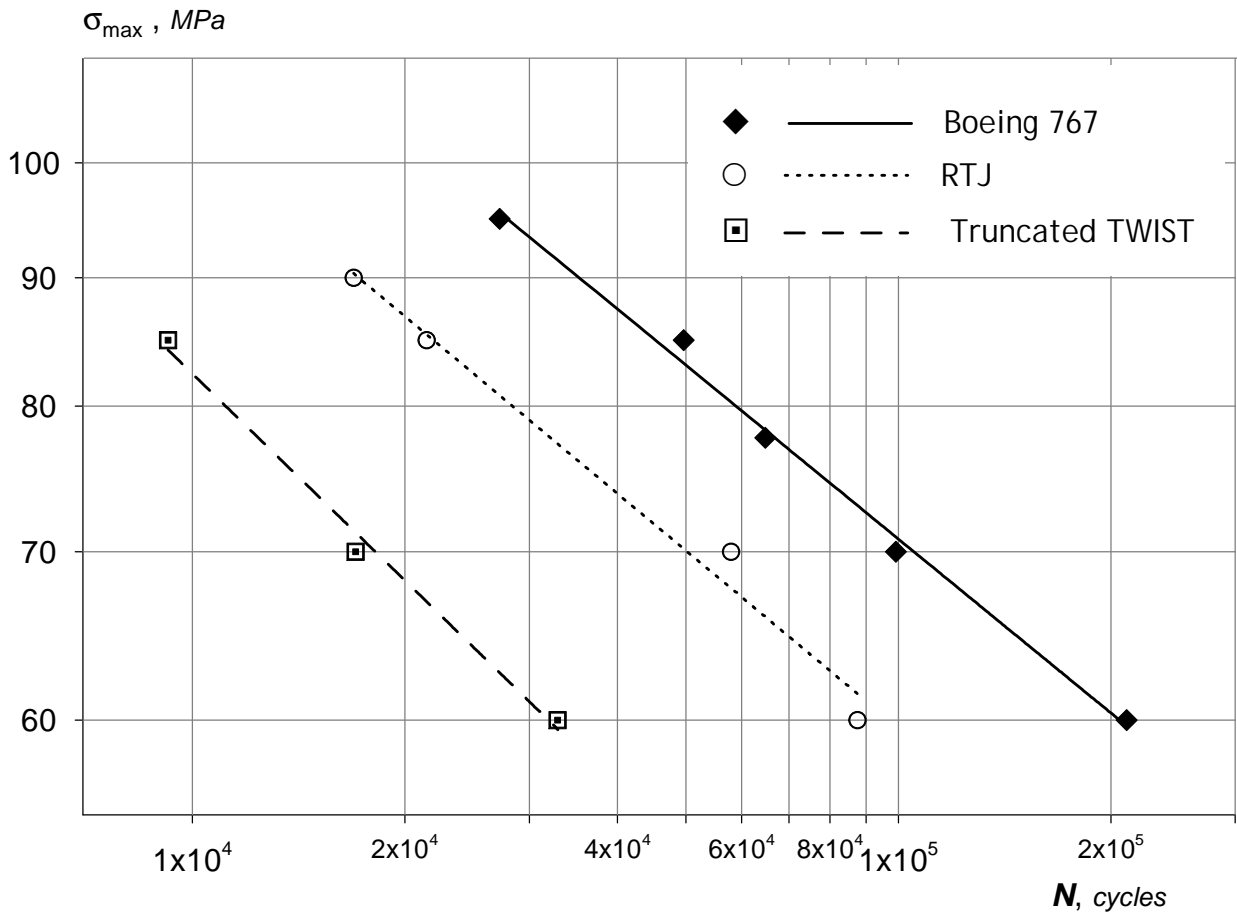


Fig. 6. Fatigue curves for D16AT specimen under random loading

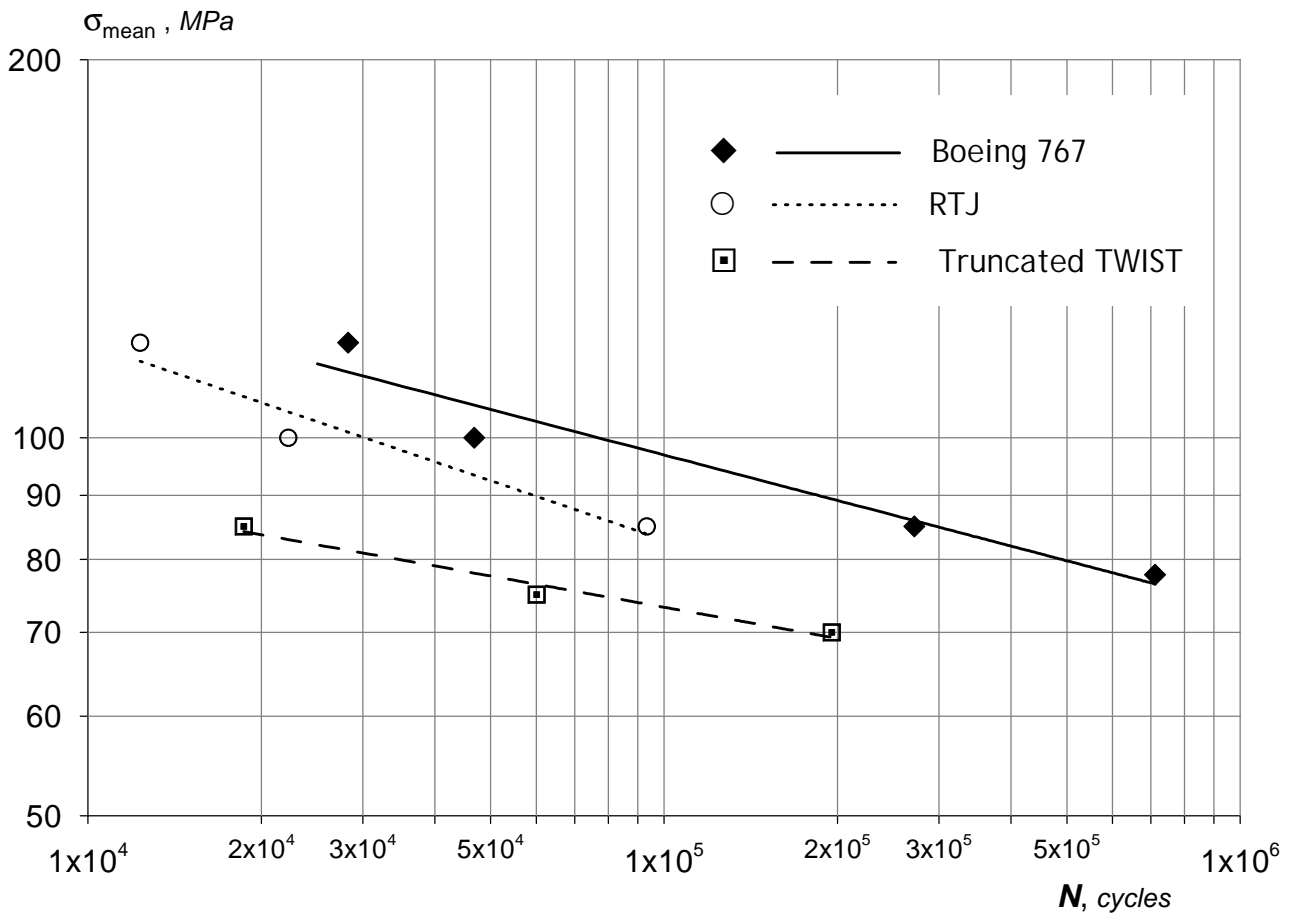


Fig. 7. Fatigue curves for 1163T7 specimens under random loading

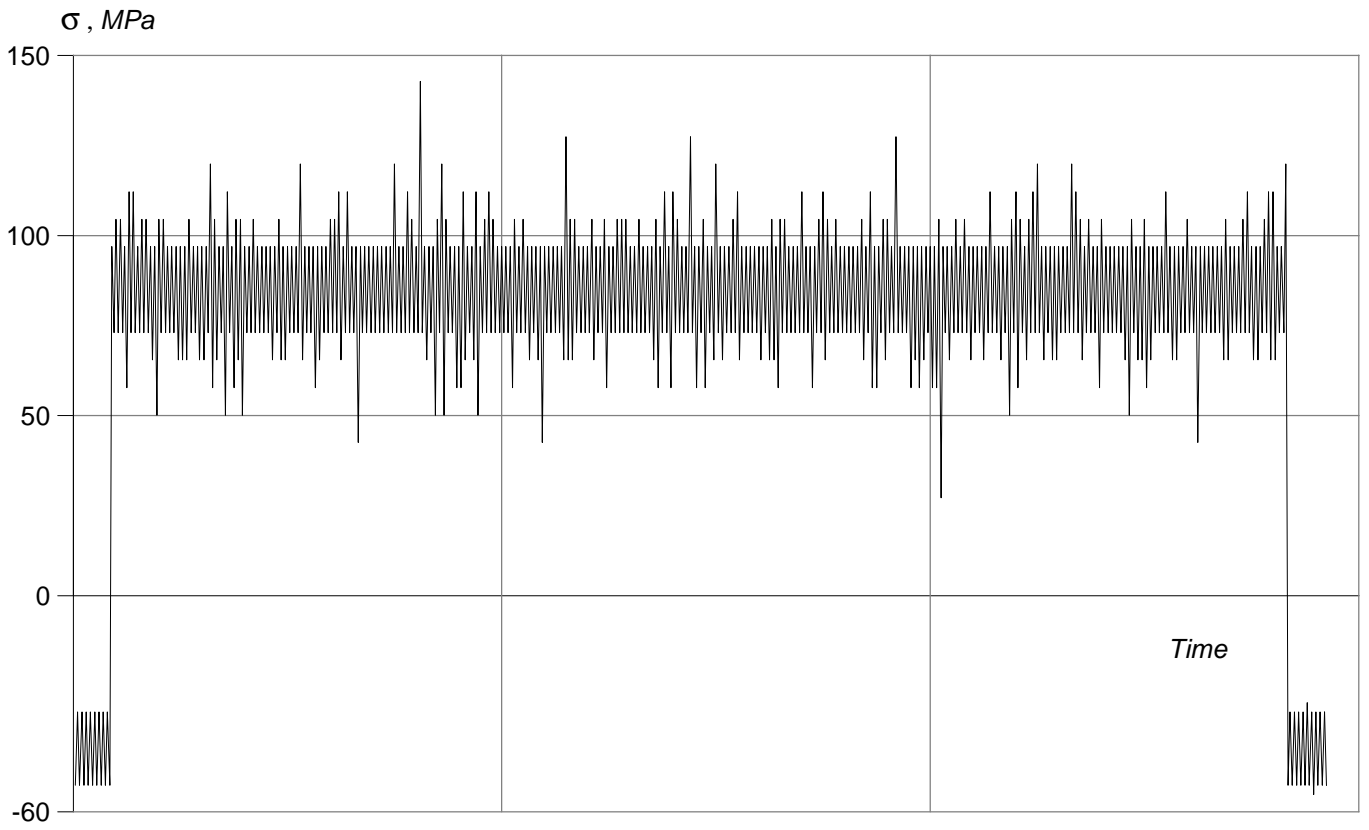


Fig. 4. Typical stress cyclogram for RTJ sequence

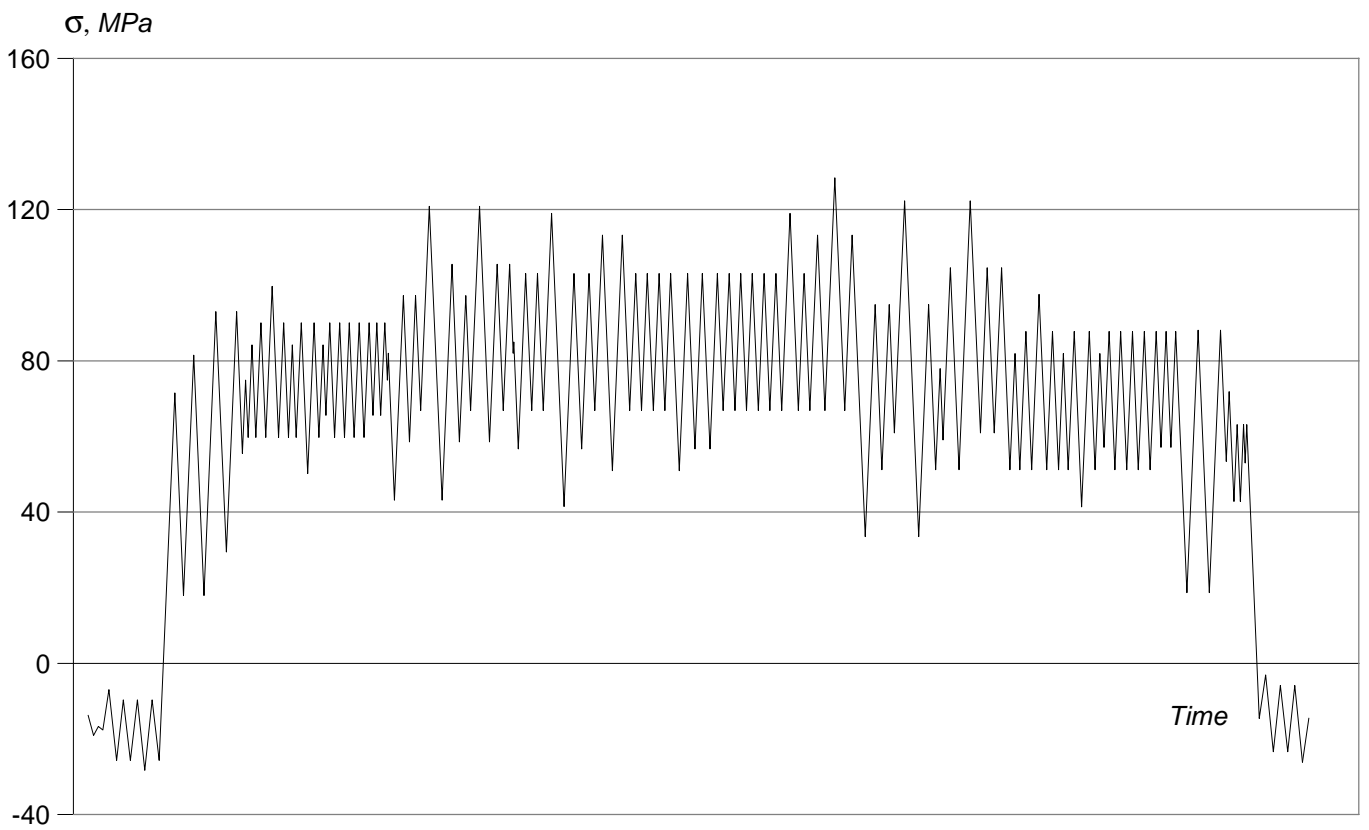


Fig. 5. Typical stress cyclogram for Boeing 767 sequence

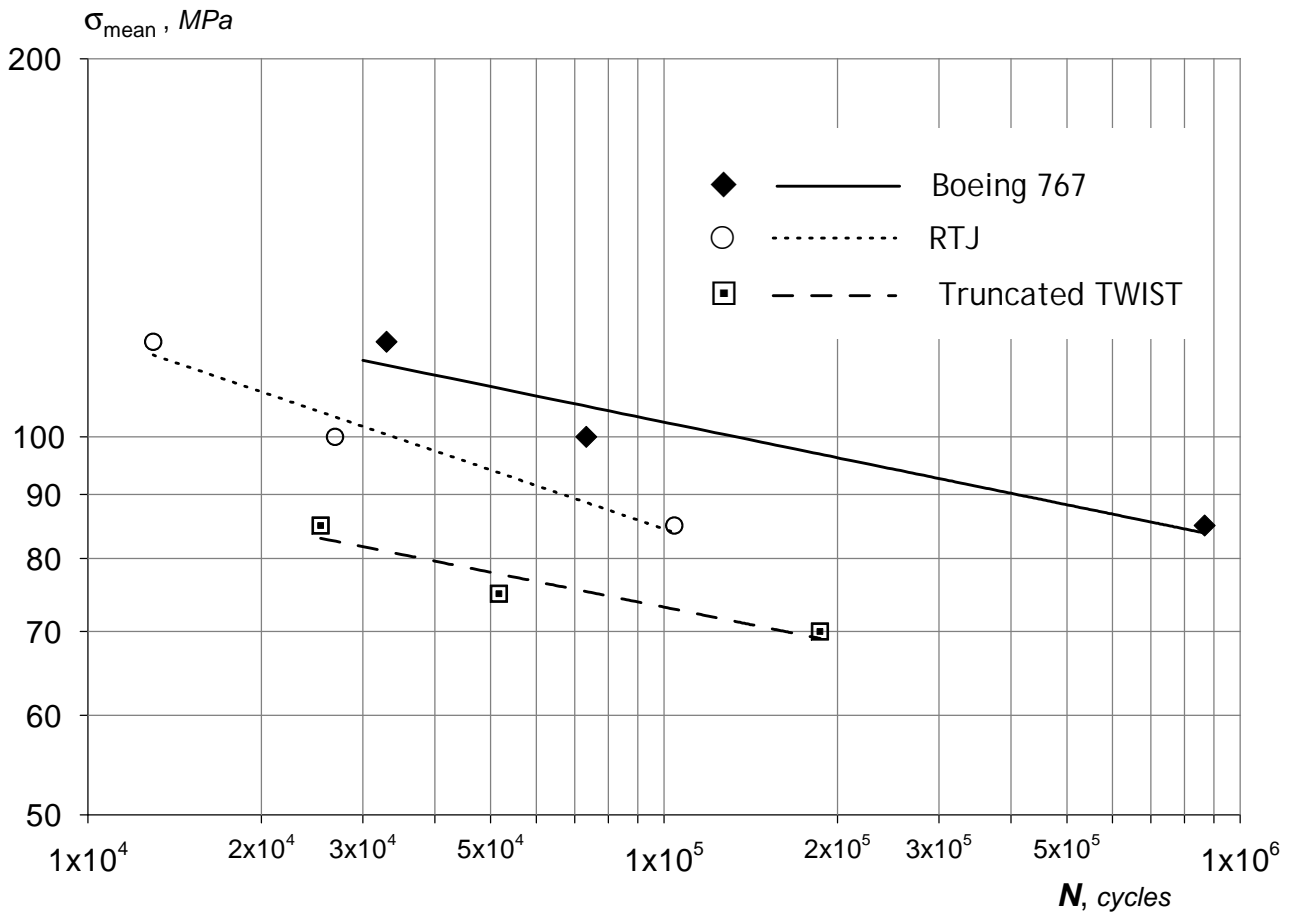


Fig. 8. Fatigue curves for 2324-T39 specimens under random loading

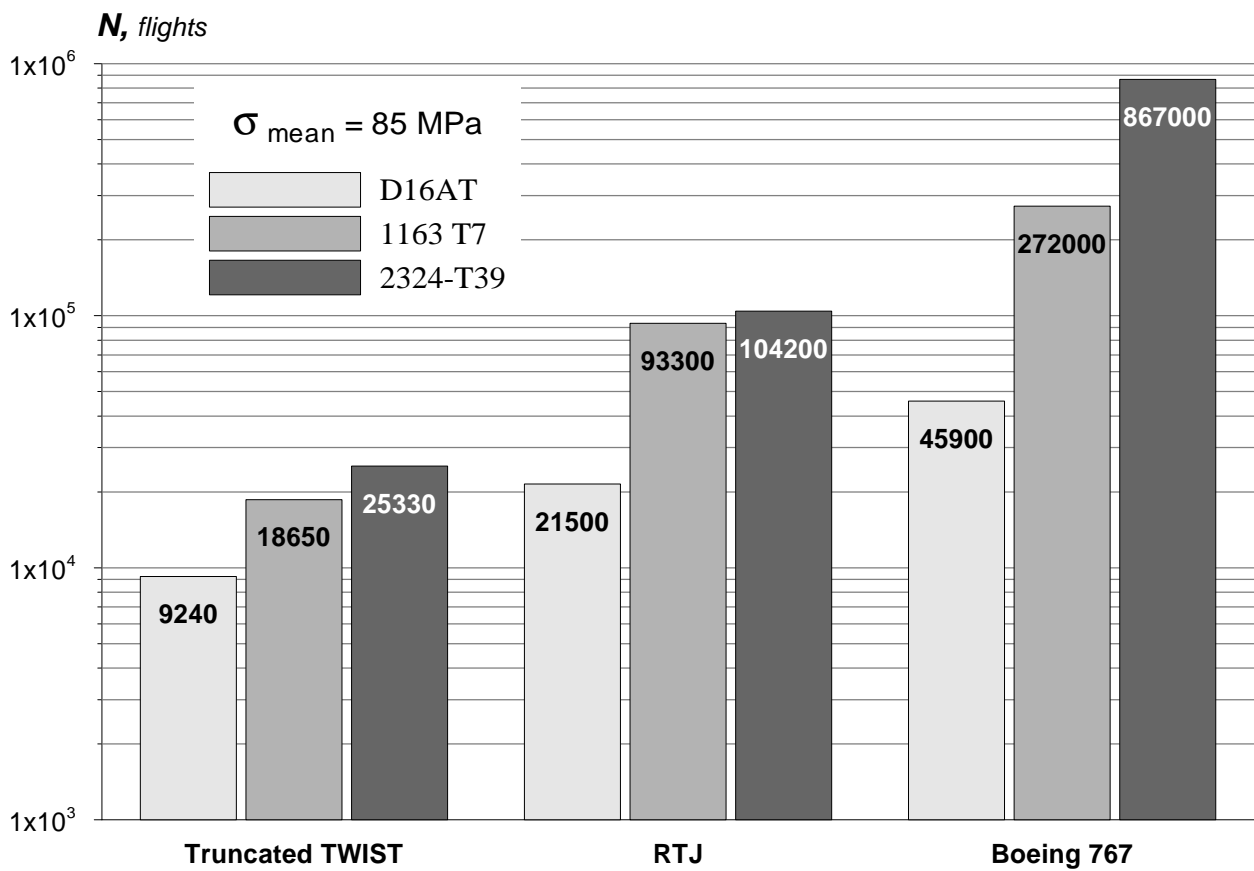


Fig. 9. Effect of loading sequence on durability of D16AT, 1163T7 and 2324-T39 specimens under random loading

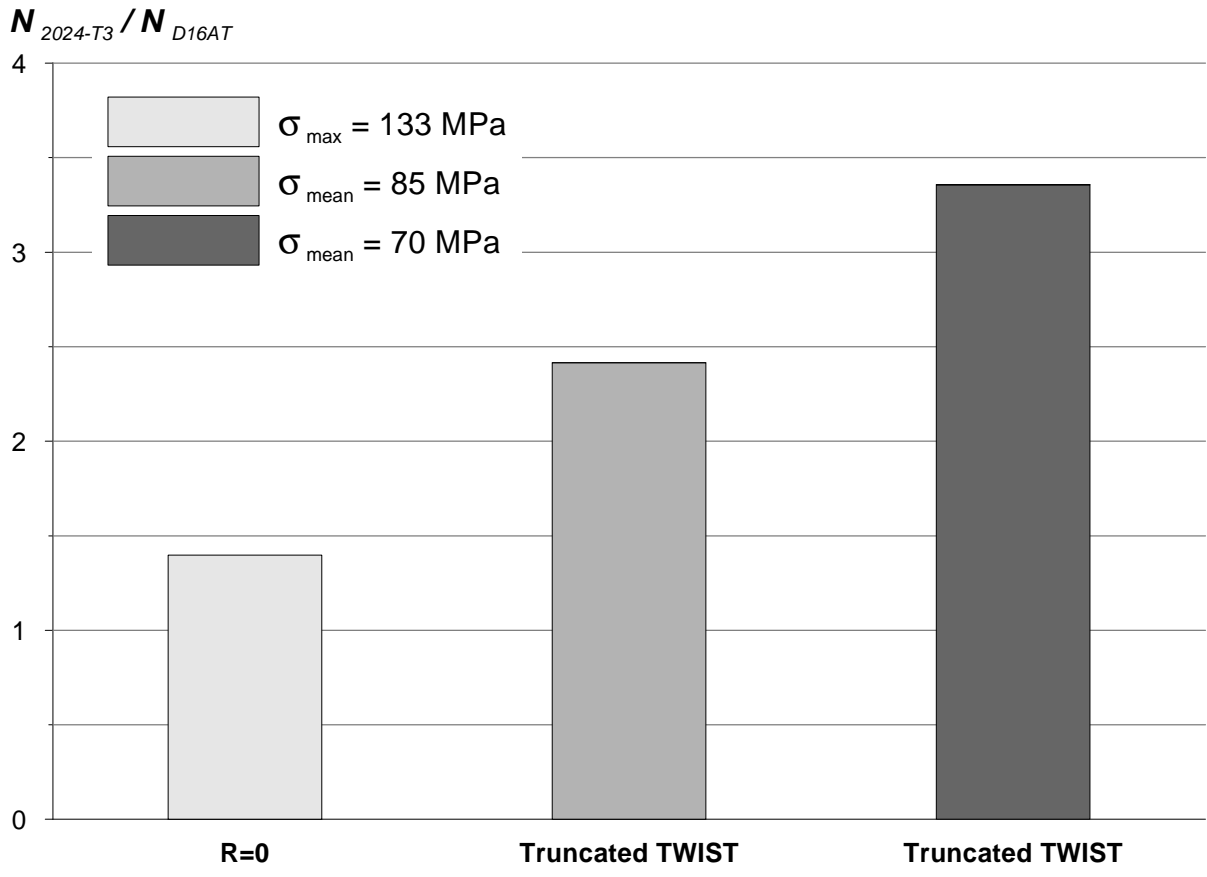


Fig. 10. Effects of loading type and level on durability of 2024-T3 and D16AT sheets

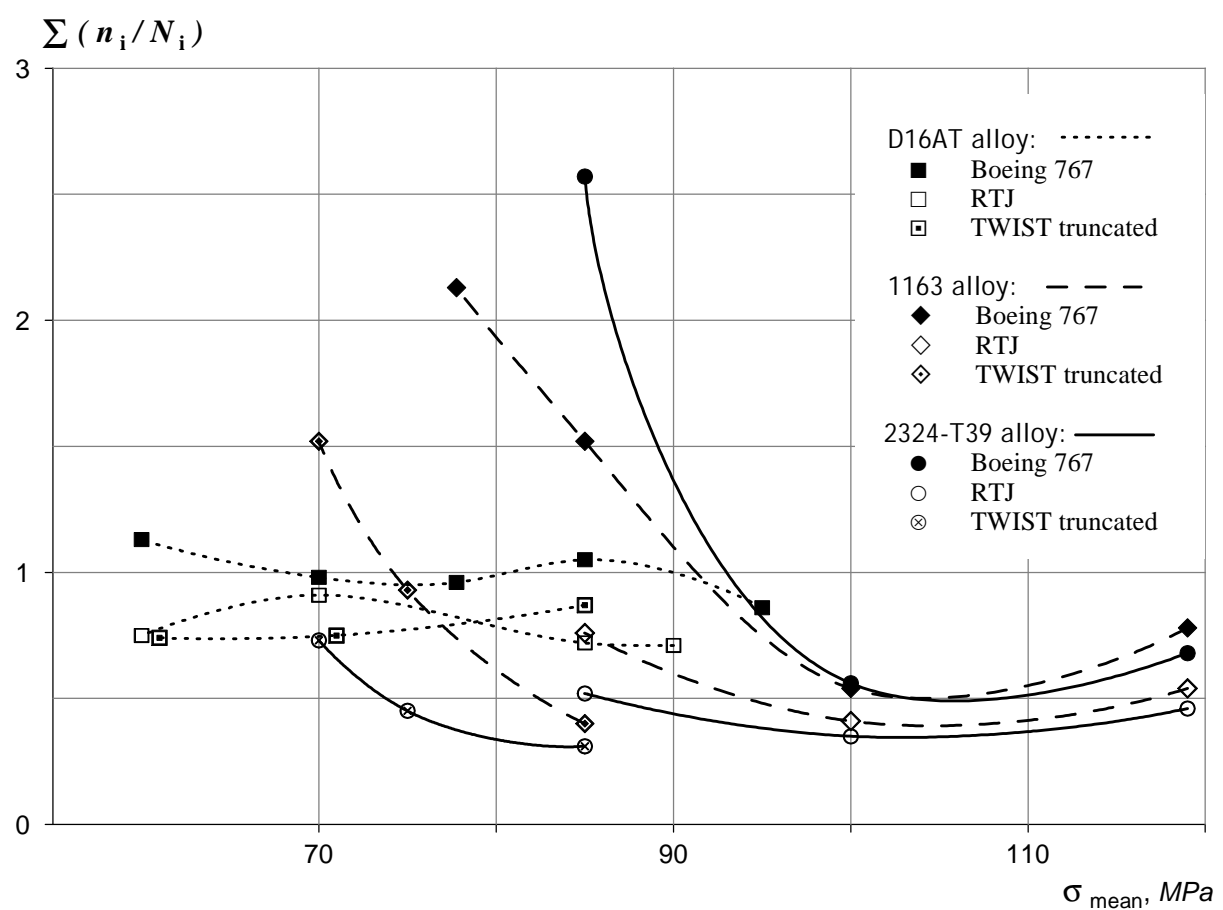


Fig. 11. Accumulated damages vs cruise mean stress

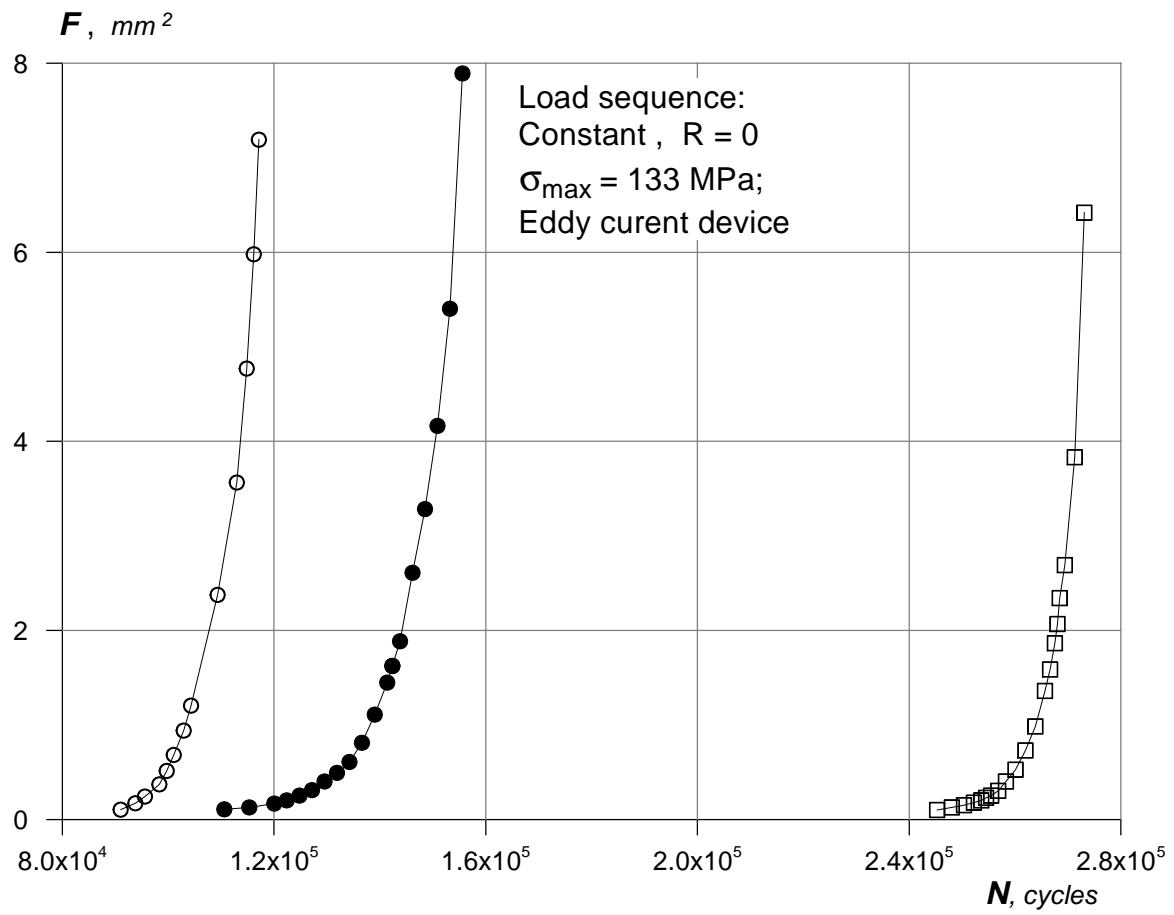


Fig. 14. Two stages of fatigue failure in 1163T7 specimens under random loading

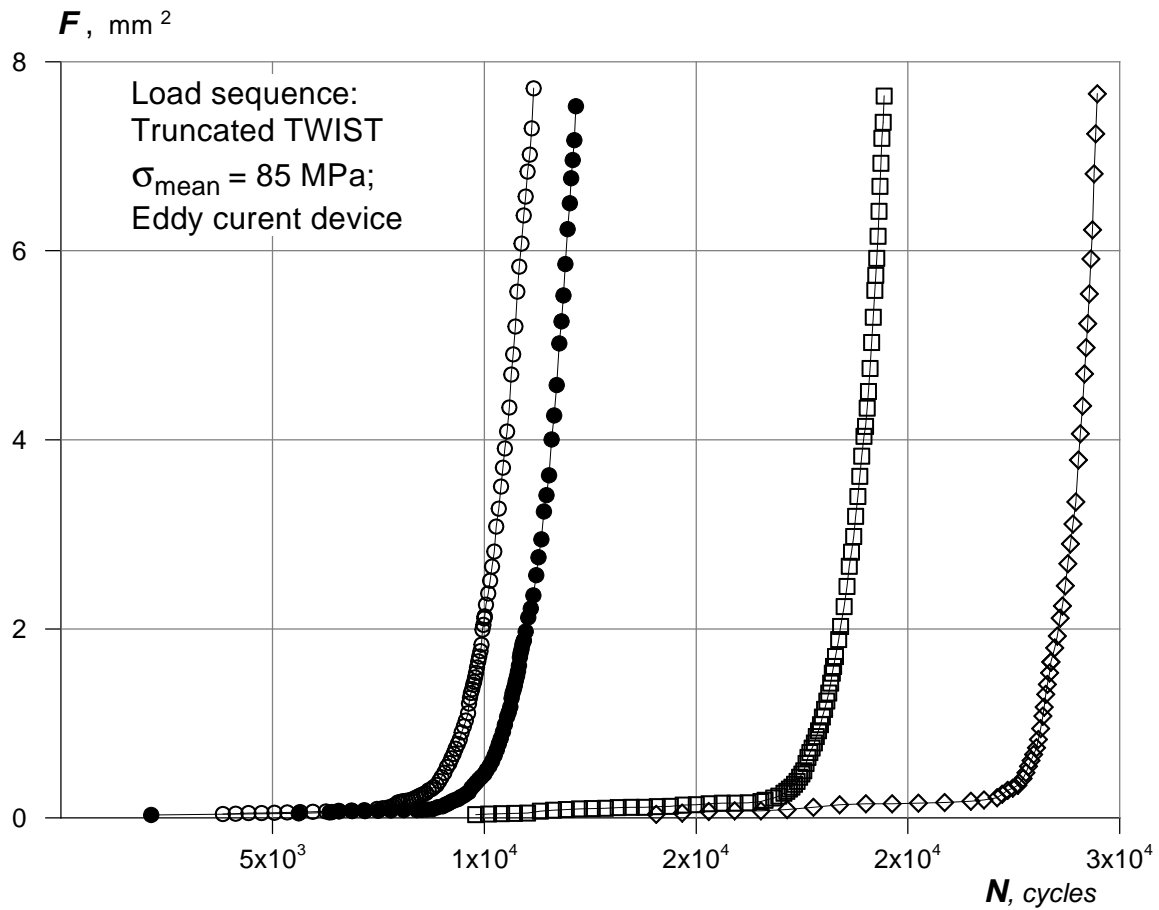


Fig. 15. Two stages of fatigue failure in 1163T7 specimens under random loading

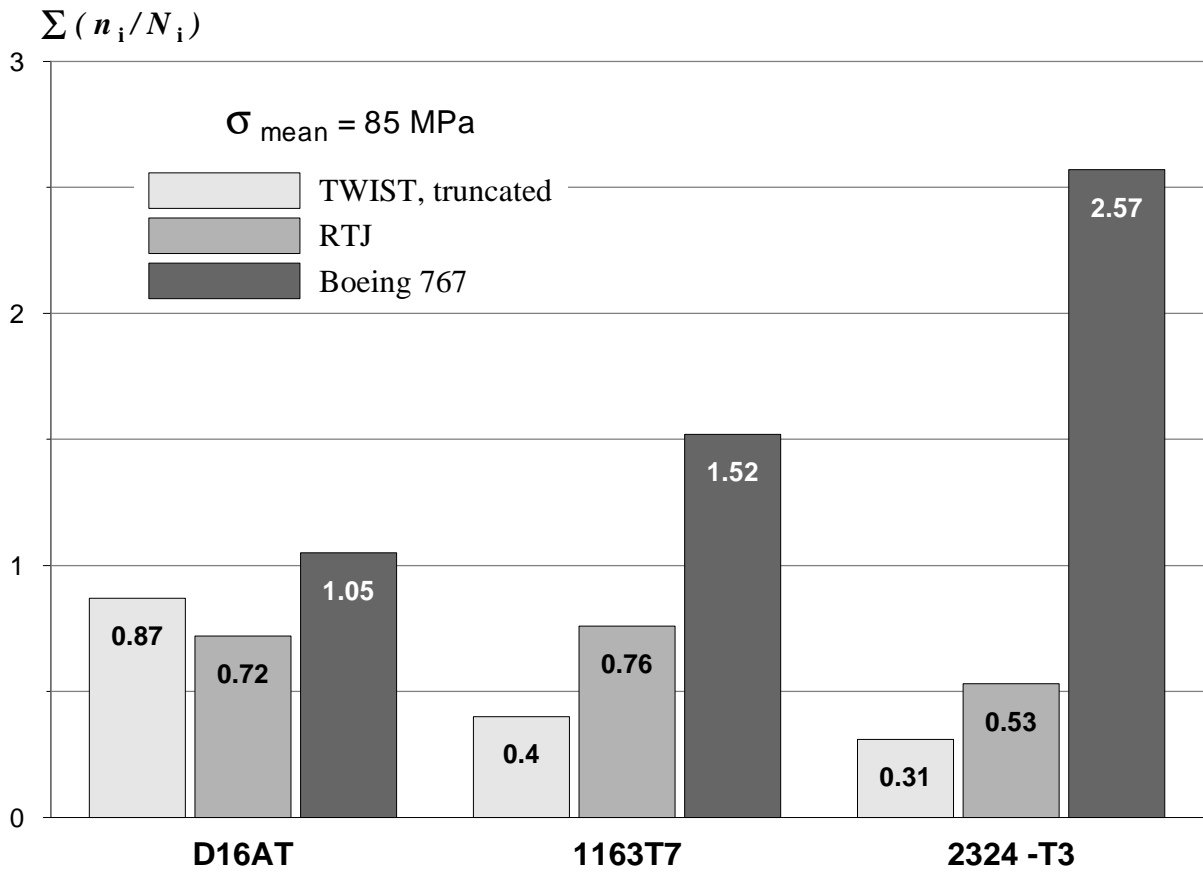


Fig. 12. Accumulated damages vs material and load sequence

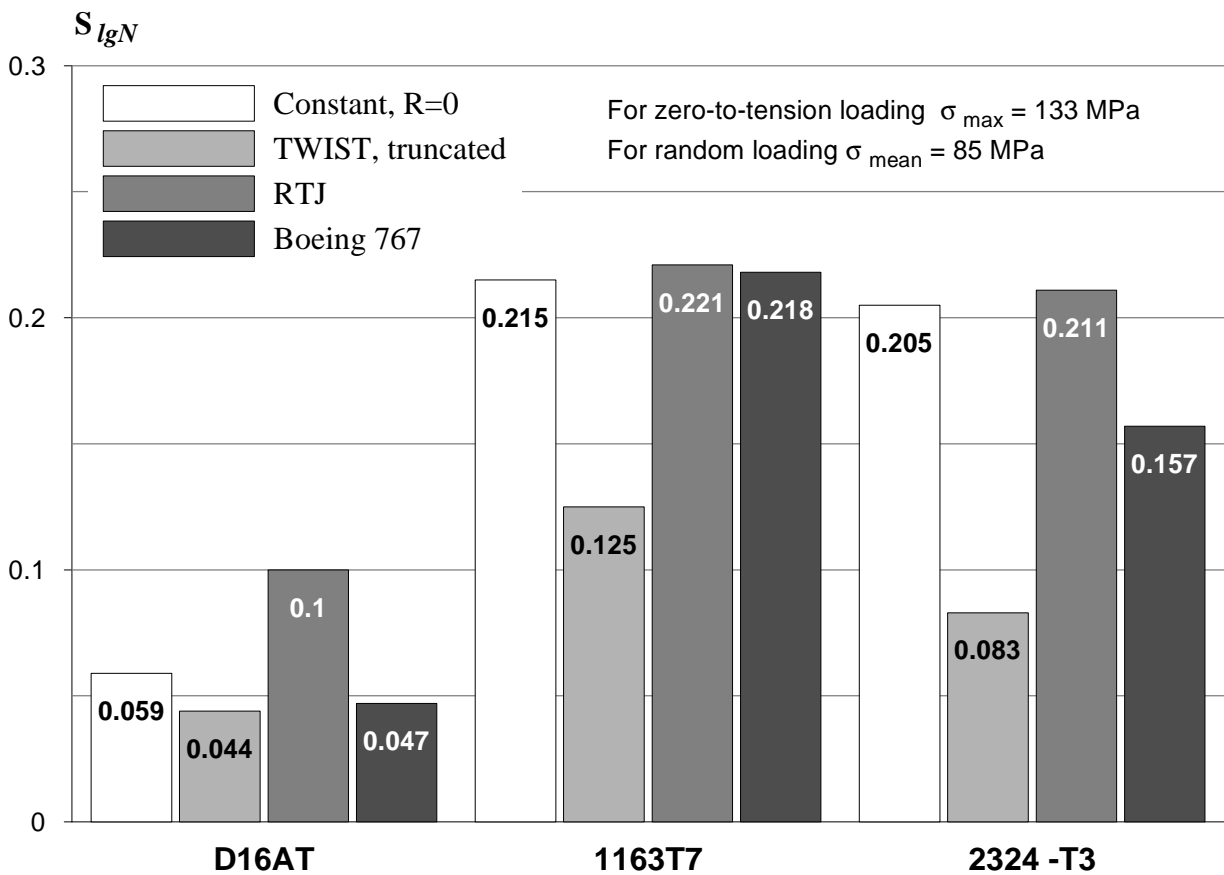


Fig. 13. Scatter of specimen durability in case of zero-to-tension and random loading

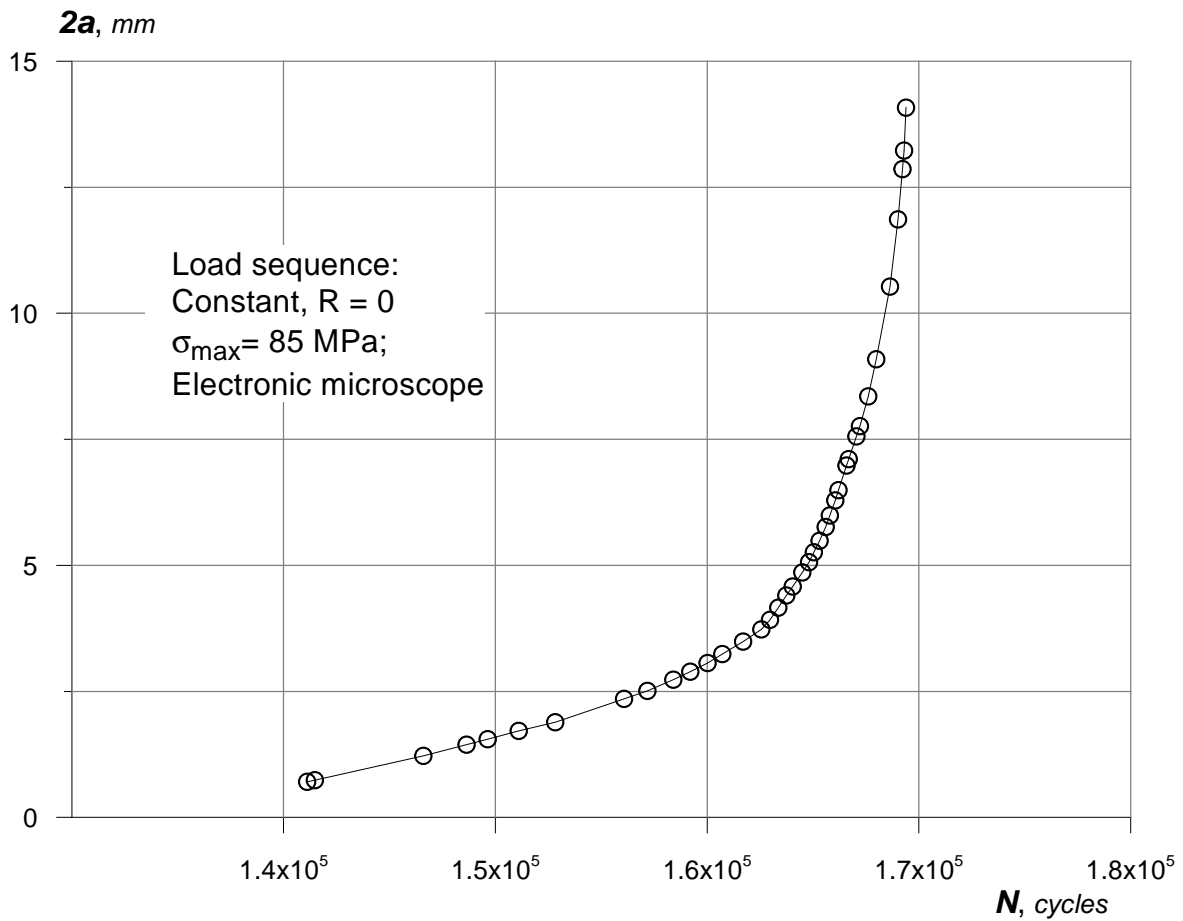


Fig. 16. Two stages of fatigue failure in 1163T7 specimens under zero-to-tension loading

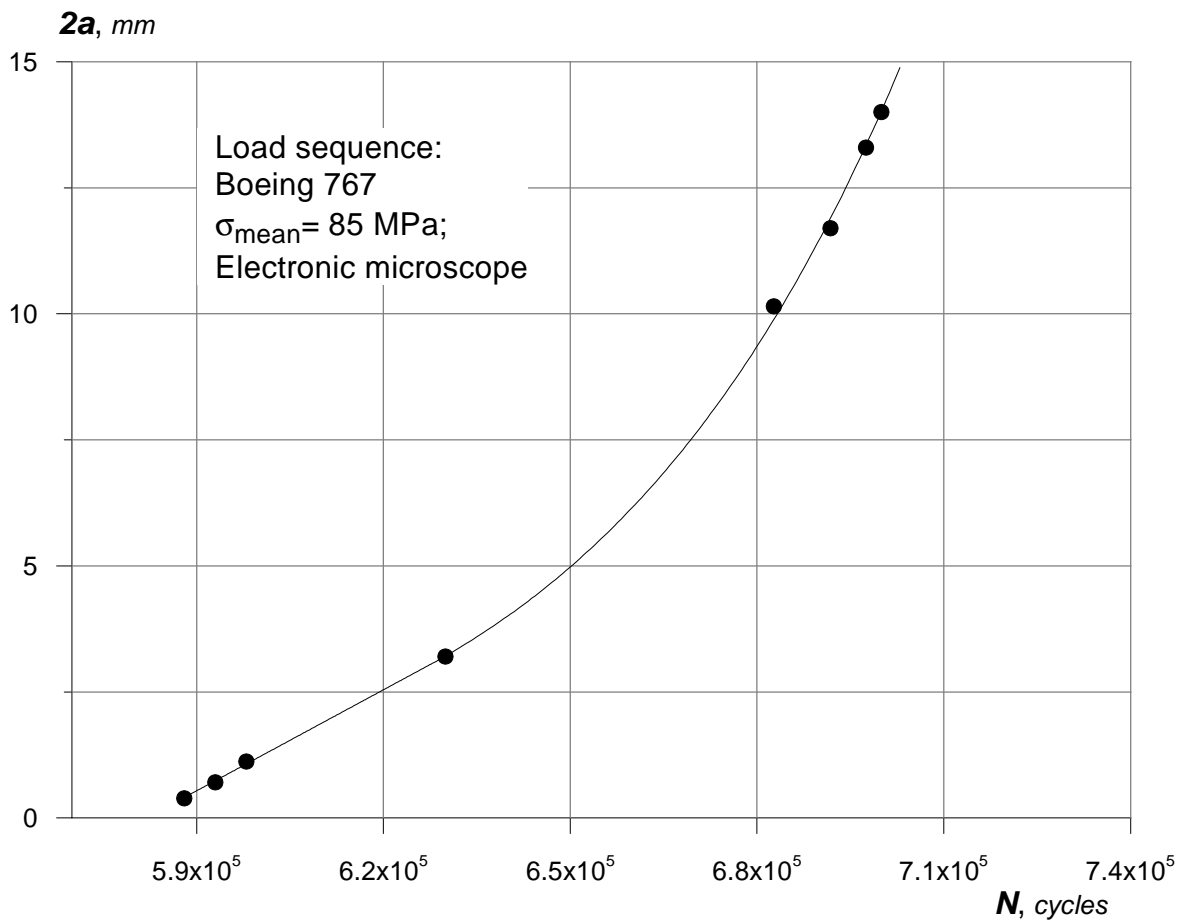


Fig. 17. Two stages of fatigue failure in 1163T7 specimens under random loading